

Novel mono-, di-, and trimethylornithine membrane lipids in northern wetland planctomycetes

Eli K. Moore^{1*}, Ellen C. Hopmans¹, W. Irene C. Rijpstra¹, Laura Villanueva¹, Svetlana N. Dedysh², Irina S. Kulichevskaya², Hans Wienk³, Frans Schoutsen⁴, Jaap S. Sinninghe Damsté¹

1. *Royal Netherlands Institute for Sea Research, Department of Marine Organic Biogeochemistry, P.O. Box 59, 1790 AB Den Burg, Texel, The Netherlands*
2. *S. N. Winogradsky Institute of Microbiology, Russian Academy of Sciences, Prospect 60-letya Otyabrya 7/2, Moscow 117312, Russia*
3. *Bijvoet Center for Biomolecular Research, Utrecht University, Padualaan 8, 3584 CH Utrecht, The Netherlands*
4. *Thermo Fisher Scientific, Takkebijsters 1, 4817 BL Breda, The Netherlands*

*corresponding author: Elisha.Moore@nioz.nl

Running Title: Methylornithine lipids in northern wetland planctomycetes

Keywords: intact polar lipids, planctomycetes, northern wetlands, ornithine, ombrotrophic

1 **Abstract**

2 Northern peatlands represent a significant global carbon store and commonly originate from
3 *Sphagnum*-moss dominated wetlands. These ombrotrophic ecosystems are rain-fed, resulting
4 in nutrient-poor, acidic conditions. Members of the bacterial phylum *Planctomycetes* are
5 highly abundant and appear to play an important role in the decomposition of *Sphagnum*-
6 derived litter in these ecosystems. High performance liquid chromatography coupled to high
7 resolution accurate mass/mass spectrometry (HPLC-HRAM/MS) analysis of lipid extracts of
8 four isolated planctomycetes from wetlands of European North Russia revealed novel
9 ornithine membrane lipids (OLs) that are mono-, di-, and trimethylated at the ϵ -nitrogen
10 position of the ornithine head group. Nuclear magnetic resonance (NMR) analysis of the
11 isolated trimethylornithine lipid confirmed the structural identification. Similar fatty acid
12 distribution between mono-, di-, and trimethylornithine lipids suggests that the three lipid
13 classes are biosynthetically linked, as in the sequential methylation of the terminal nitrogen in
14 phosphatidylethanolamine to produce phosphatidylcholine. The mono-, di-, and
15 trimethylornithine lipids described here represent the first report of methylation of the
16 ornithine head groups in biological membranes. Various bacteria are known to produce OLs
17 under phosphorus limitation, or fatty acid hydroxylated OLs under thermal or acid stress. The
18 sequential methylation of OLs leading to a charged choline-like moiety in the
19 trimethylornithine lipid head group, may be an adaptation to provide membrane stability in
20 acidic conditions without the use of scarce phosphate in nutrient-poor ombrotrophic wetlands.

INTRODUCTION

21
22 Northern peatlands are a significant global carbon store accounting for approximately
23 one third of global soil organic carbon, despite only making up 3% of the world's land area
24 (1-3). Areas with peatland development correspond closely to the distribution of *Sphagnum*
25 moss-dominated bogs (4). Ombrotrophic, nutrient-poor, acidic conditions of these wetlands,
26 along with low temperatures, and the presence of decay resistant phenolic compounds and
27 waxes in *Sphagnum* tissues, lead to low decomposition rates of *Sphagnum*-derived litter (5-9).
28 Consequently, carbon sequestration due to net primary production in *Sphagnum*-dominated
29 bogs is greater than the amount of carbon lost to the atmosphere by decomposition of dead
30 organic matter, making northern wetlands an important global carbon sink (10-12).

31 The composition of the bacterial community in *Sphagnum* peat bogs is fundamentally
32 different from the community that decomposes plant debris in eutrophic systems at neutral pH
33 (13-15). It has been recently discovered that *Planctomyces* make up an important part of the
34 bacterial population responsible for *Sphagnum* decomposition, accounting for up to 14% of
35 total bacterial cells (14, 16-17). Cell numbers of planctomyces have been observed to
36 increase in the late stages of *Sphagnum* debris degradation (14). All currently described peat-
37 inhabiting planctomyces are capable of degrading various heteropolysaccharides, while only
38 one of them, *Telmatocola sphagniphila*, possesses weak cellulolytic potential (18-22). The
39 addition of available nitrogen to cellulose-amended *Sphagnum* peat degradation experiments
40 resulted in a decrease of the relative abundance of *Planctomyces* in the total microbial
41 community (15). This suggests that planctomyces in ombrotrophic wetlands are highly
42 adapted to nutrient-poor conditions and contribute mainly to final stages of plant litter
43 decomposition.

44 Various studies have predicted that northern peatlands will change from atmospheric
45 carbon sink to source in future climate warming scenarios further accelerating global warming

46 (23-24). High temperature sensitivity of soil respiration at low temperatures (25-26) makes
47 these ecosystems especially susceptible to climate impacts. It has been observed that 1°C
48 temperature increase for *in situ* subarctic peatland climate manipulation experiments
49 accelerated total ecosystem respiration rates by 50 to 60% depending on the season (27).
50 Heterotroph-dominated subsurface peat respiration accounted for at least 70% of the increased
51 respiration rates, demonstrating that climate change may have a major impact on the
52 microbial recycling of stored organic carbon in northern wetlands. Therefore, it is important
53 to study the microbial communities involved in the degradation of *Sphagnum*-derived material
54 and the mechanisms of their adaptation to ombrotrophic conditions including *Planctomyces*,
55 of which little is known.

56 Cell membranes are built out of intact polar lipids (IPLs), which consist of a polar
57 head group connected to hydrophobic carbon chain tail groups. IPLs can be useful biomarker
58 molecules because their molecular structures can be taxonomically and environmentally
59 specific, and are thought to represent living biomass (28-29). Given the unique environmental
60 niche which these *Sphagnum*-bog *Planctomyces* occupy, their membranes may be adapted
61 to these conditions and contain unique biomarker lipids that could be used to further
62 investigate the role of *Planctomyces* in this globally important ecosystem, and indicate how
63 they may respond to environmental change. Indeed, all planctomycete strains that have been
64 isolated from *Sphagnum* wetlands of Northern Russia contained polar membrane lipids of
65 unknown structure (19, 21-22), which might have biomarker potential. Here we describe the
66 isolation and characterization of several of these unidentified polar membrane lipids. High
67 resolution accurate mass orbitrap mass spectrometry (HRAM/OT/MS) combined with nuclear
68 magnetic resonance (NMR) revealed a series of ornithine lipids with increasing head group
69 methylation. These lipids appear to be common in planctomyces from this unique
70 environment.

71 **MATERIALS AND METHODS**

72 **Strains and culture conditions.** The planctomycetes *S. acidiphila* MOB10^T (DSM
73 18658^T), *S. rosea* S26^T (DSM 23044^T), *T. sphagniphila* SP2^T and OB3 (DSM 23888^T), and
74 *Gemmata*-like strain SP5 were isolated from the upper oxic layer (0-10 cm) of acidic peat
75 collected from wetlands of European North Russia and described by Kulichevskaya *et al.* (19,
76 21-22, Supplementary Material – Appendix I). *S. acidiphila* MOB10^T and *S. rosea* S26^T were
77 grown in liquid medium M31 (modification of medium 31 described by Staley *et al.* (30)
78 containing (g per liter of distilled water): KH₂PO₄, 0.1; Hutner's basal salts, 20 ml; N-
79 acetylglucosamine, 1.0; peptone, 0.1; yeast extract, 0.1; pH 5.8. *T. sphagniphila* SP2^T and
80 OB3 as well as *Gemmata*-like strain SP5 were grown in liquid medium M1N of the following
81 composition (gram per liter of distilled water): KH₂PO₄, 0.1; (NH₄)₂SO₄, 0.1; MgSO₄ x 7H₂O,
82 0.1; CaCl₂ x 2H₂O, 0.02; yeast extract, 0.1; glucose, 0.25; 1 ml of trace element solution '44'
83 and 1 ml Staley's vitamin solution (30); pH 5.5. Cultivation was done in 500-ml flasks
84 containing 100 ml medium. Cultures were incubated at 22°C on a shaker and harvested in the
85 late exponential growth phase. Biomass was collected and freeze dried for extraction and
86 analysis.

87 **Lipid extraction.** Lipids were extracted from freeze dried biomass of each culture by
88 a modified Bligh & Dyer method (31). For structural comparison, lipids were also extracted
89 from freeze dried biomass of the Bacterioidete *Flavobacterium johnsoniae*, known to contain
90 high concentration of ornithine lipids. Freeze dried biomass of each culture was fully
91 submerged and extracted three times in methanol/dichloromethane/phosphate-buffer
92 (MeOH/DCM/P-buffer, 2/1/0.8, v/v/v) extraction solvent for 10 min in an ultrasonic bath (P-
93 buffer: 8.7 g K₂PO₄ L⁻¹ bi-distilled water adjusted to pH 7–8 with 1 N HCl). Extracts were
94 centrifuged for 2 min at 1400 g to separate DCM phase from the MeOH/P-buffer phase, and
95 the lower DCM layer was pipetted into a separate vial. The MeOH/P-buffer layer was

96 washed twice more with DCM, centrifuged, and the resulting DCM layers were pipetted into
97 the same vial as the original DCM layer. DCM was removed under a stream of nitrogen, the
98 residue was dissolved in injection solvent (hexane:2-propanol:H₂O, 718:271:10, v/v/v), and
99 filtered through a 0.45 μ m, 4 mm diameter TrueTM Regenerated Cellulose syringe filter
100 (Grace Davison) prior to injection. Extracts were stored at -80°C until analysis.

101 **HPLC-MS analysis.** Intact polar lipids were analyzed by high performance liquid
102 chromatography-electrospray ionization/ion trap mass spectrometry (HPLC-ESI/IT/MS)
103 according to Sturt *et al.* (28) with some modifications (32). Briefly, an Agilent 1200 series
104 HPLC, with thermostatted auto-injector, was coupled to a Thermo LTQ XL linear ion trap
105 mass spectrometer with Ion Max source and ESI probe (Thermo Scientific, Waltham, MA).
106 Typical lipid extract injection concentration was 2 mg/ml, and the injection volume was 10 μ l.
107 Chromatographic separation was performed on a Lichrosphere diol column (250 mm \times 2.1
108 mm, 5 μ m particles; Grace Alltech Associates Inc.). Elution was achieved with (A) hexane-2-
109 propanol-formic acid-14.8 M aqueous NH₃ (79:20:0.12:0.04, v/v/v/v) and (B) 2-propanol-
110 water-formic acid-14.8 M aqueous NH₃ (88:10:0.12:0.04, v/v/v/v) starting at 10% B, followed
111 by a linear increase to 30% B in 10 min, followed by a 20 min hold, and a further increase to
112 65% B at 45 min. Flow rate was 0.2 ml min⁻¹, total run time was 60 min, followed by a 20
113 min re-equilibration period. The lipid extracts were analyzed by scanning a mass range of m/z
114 400-2000 in positive ion mode, followed by data-dependent, dual stage tandem MS (MS²), in
115 which the four most abundant masses in the mass spectrum were fragmented successively
116 (normalized collision energy, 25; isolation width, 5.0; activation Q, 0.175). Each MS² was
117 followed by data dependent, triple-stage tandem MS (MS³), where the base peak of the MS²
118 spectrum was fragmented under identical fragmentation conditions as described for MS². The
119 ion trap MS was calibrated using the Thermo Scientific LTQ ESI Positive Ion Calibration
120 Solution (contains mixture of caffeine, MRFA, and Ultramark 1621 in an acetonitrile/

121 methanol/acetic solution). Performance of the HPLC-ESI/IT/MS was monitored by regular
122 injections of platelet-activating factor (PAF) standard (1-O-hexadecyl-2-acetyl-*sn*-glycero-3-
123 phosphocholine). Relative differences in ornithine and methylornithine IPL ionization and
124 instrument response were corrected for by use of external standards (Avanti Polar Lipids, Inc.:
125 1,2-dipalmitoyl-*sn*-glycero-3-phosphoethanolamine; 1,2-dipalmitoyl-*sn*-glycero-3-
126 phosphoethanolamine-N-methyl; 1,2-dipalmitoyl-*sn*-glycero-3-phosphoethanolamine-N,N-
127 dimethyl; 1,2-dipalmitoyl-*sn*-glycero-3-phosphocholine).

128 HPLC-HRAM/OT/MS analysis of the *T. sphagniphila* extract was accomplished on a
129 3000 UltiMate series LC with thermostated auto-injector coupled to a Q Exactive high
130 resolution accurate mass Orbitrap mass spectrometer (Thermo Scientific). Chromatographic
131 conditions and column were the same as described above for HPLC-ESI/IT/MS. Positive ion
132 ESI settings were: capillary temperature, 275°C; sheath gas (N₂) pressure, 35 arbitrary units
133 (AU); auxiliary gas (N₂) pressure, 10 AU; spray voltage, 4.0 kV; probe heater temperature,
134 300°C; S-lens 50 V. Target lipids were analyzed with a mass range of *m/z* 400–1000
135 (resolution 70,000), followed by data-dependent tandem MS (MS²; resolution 17,500), in
136 which the five most abundant masses in the mass spectrum were fragmented successively
137 (normalized collision energy, 35; isolation width, 1.0). The Q Exactive was calibrated within
138 a mass accuracy range of 1 ppm using the Thermo Scientific Pierce LTQ Velos ESI Positive
139 Ion Calibration Solution (contains mixture of caffeine, MRFA, Ultramark 1621, and n-
140 butylamine in an acetonitrile/methanol/acetic solution).

141 **Fatty acid analysis.** An aliquot of *T. sphagniphila* Bligh & Dyer extract was
142 hydrolyzed with 1.5 N HCl in MeOH by reflux for 3 hr. The hydrolysate was adjusted to pH
143 4 with 2 N KOH-MeOH (1:1, v/v). Water was added to give a final ratio of 1:1 H₂O-MeOH,
144 and then extracted three times with DCM. The DCM fractions were collected and dried over
145 sodium sulfate. The extract was then methylated with diazomethane (33), followed by

146 silylation in pyridine with N,O-bis(trimethylsilyl)trifluoro-acetamide (BSTFA) at 60°C for 20
147 min. Methylated-silylated extracts were then dissolved in ethyl acetate for gas
148 chromatography/mass spectrometry (GC/MS) analysis.

149 **GC and GC-MS.** GC was performed using a Hewlett-Packard (HP6890) gas
150 chromatograph equipped with an on-column injector and a flame ionization detector.
151 Chromatography was accomplished using a fused silica capillary column (25 m × 0.32 mm)
152 coated with CP Sil-5 CB (film thickness, 0.12 μm) with helium as the carrier gas. The
153 samples were injected at 70°C, and the oven temperature was ramped to 130°C at 20°C/min
154 and then 4°C/min to 320°C, at which it was held for 10 min. GC-MS was performed on a
155 Finnigan Trace Ultra gas chromatograph interfaced with a Finnigan Trace DSQ mass
156 spectrometer operated at 70 eV with a mass range of m/z 40 to 800 and a cycle time of 1.7 s
157 (resolution, 1,000). The gas chromatograph employed a fused silica capillary column as
158 described for GC, and also used helium as the carrier gas. The same temperature program
159 was used as with GC.

160 **Target lipid isolation.** Target lipids were isolated from extracts using an Agilent
161 Technologies (Santa Clara, CA) 1100 series LC equipped with an auto-injector, and a fraction
162 collector (Foxy Jr., Isco, Inc., Lincoln, NE). A first isolation was achieved on a semi-
163 preparative Lichrosphere diol column (10 × 250 mm, 5 μm; Grace Alltech Associates Inc.)
164 according to Boumann et al. (34) with the same gradient program as described above for
165 HPLC-ESI/IT/MS, but at a flow rate of 3 ml min⁻¹. Typical injection volume was 200 μL
166 containing up to 2 mg material. Column effluent was collected in 1 min fractions, which were
167 screened for the presence of target lipids by flow injection analysis cf. Smittenberg *et al.* (35)
168 using the ESI/IT/MS (5 μl injection of each fraction, ESI source settings same as described
169 above for HPLC-ESI/IT/MS with a scan range of m/z 400–2000). Fractions containing target
170 lipids were pooled and further purified on a second Lichrosphere diol column (4.6 × 250 mm,

171 5 μm ; Grace Alltech Associates Inc.). Typical injection volumes were 65 μl containing up to
172 0.65 mg of material. Lipids were eluted using the identical gradient program and conditions
173 as described above for HPLC-ESI/IT/MS, but with slightly modified mobile phases such that
174 neither mobile phases A or B contained NH_3 or formic acid, at a flow rate of 1 ml min^{-1} .
175 Column effluent was collected in 15 sec fractions and screened as described above. Fractions
176 containing target lipids were again combined and elution solvent was removed under a stream
177 of nitrogen. Purity was assessed by HPLC-ESI/IT/MS as described above for IPL analysis.
178 Isolated lipids were stored at -80°C prior to further analysis.

179 **Nuclear Magnetic Resonance.** Purified lipids were dissolved in 99.9% CDCl_3 at a
180 concentration of 1.5 $\mu\text{mol ml}^{-1}$, and NMR experiments were performed at 298K on Bruker
181 600 MHz and 750 MHz Avance spectrometers, equipped with triple resonance TXI probes,
182 and running under TOPSPIN 2.1. The 600 MHz 1D ^1H , and ^1H -decoupled 1D ^{13}C and
183 DEPT-135 experiments were recorded with spectral widths/offsets of 24 ppm/6 ppm, 200
184 ppm/100 ppm, and 200 ppm/100 ppm, and with 16k, 1k and 1k complex points, respectively.
185 The 14×14 ppm 2D COSY, TOCSY and NOESY experiments were performed at 750 MHz
186 with 512×512 complex points and offset frequency of 6 ppm. Mixing times were 60 ms and
187 250 ms for TOCSY and NOESY, respectively. The (^1H , ^{13}C)-HSQC and (^1H , ^{13}C)-HMBC
188 experiments were recorded at 600 MHz with spectral widths/offset 14/6 ppm for proton and
189 200/100 ppm for carbon-13. Spectra were calibrated with respect to internal residually
190 protonated CHCl_3 at 7.24 ppm (^1H) and 77.0 ppm (^{13}C).

RESULTS

191
192 **Unknown IPLs detected by HPLC-ESI/IT/MS.** Intact polar lipid analysis of four
193 recently described planctomycete strains from Russian peatlands revealed known and
194 unknown membrane lipid structures. In addition to the commonly observed lipid classes
195 phosphatidylcholine (PC), phosphatidylglycerol (PG), phosphatidic acid (PA),
196 phosphatidylethanolamine (PE), monomethylphosphatidylethanolamine (MMPE),
197 dimethylphosphatidylethanolamine (DMPE), and amino acid-containing ornithine lipids (Fig.
198 1; OL, phosphorus free membrane lipids found only in bacteria), three groups of unknown
199 lipids (I-III) were observed in the lipid extracts from each of the four analyzed planctomycete
200 species by HPLC-ESI/IT/MS polar lipid analysis in agreement with previously reported
201 results by Kulichevskaya *et al.* (19, 21-22) (Fig. 2). Group I, II, and III lipids made up the
202 majority of IPLs in *T. sphagniphila* and *Gemmata*-like SP5 extracts, and a large portion of
203 IPLs in *S. rosea* and *S. acidiphila* (Table 1). The lipid extract from *T. sphagniphila* contained
204 the greatest amount of these unknown lipids and the identification efforts, therefore, focused
205 on this species. In the *T. sphagniphila* extract, each of the three unknown lipid clusters
206 showed 5 dominant mass signals separated by 14 Th. The main five observed masses in
207 group I (m/z 637, 651, 665, 679, and 693) were each 14 Th lighter than the five masses in
208 group II (m/z 651, 665, 679, 693, and 707), and the masses in group II were 14 Th lighter than
209 the masses in group III (m/z 665, 679, 693, 707, and 721).

210 Each of the unknown lipid groups displayed ornithine-like MS fragmentation but
211 different fragmentation products. Typical ornithine lipid MS² fragmentation involves the loss
212 of a water molecule and a fatty acyl chain ($R_2CH=C=O$), followed by the loss of the second
213 fatty acid as a ketene ($R_1CH=C=C=O$) during MS³ fragmentation resulting in a diagnostic
214 product at m/z 115 ($C_5H_{11}N_2O$) representing the ornithine head group (36). Ion trap
215 fragmentation of lipid groups I, II, and III followed a similar pattern, but resulted in different

216 fragmentation products in MS³, suggesting a similar general IPL structure to ornithine lipids
217 but with a different polar head group. Compounds in group I yielded a product of m/z 129,
218 after MS³ fragmentation. Group II was characterized by multiple low abundance MS³
219 fragmentation products at m/z 100, 115, 144, 161, and 185. Lipids in cluster III displayed
220 slightly different fragmentation behavior with the apparent loss of a fatty acid, followed by
221 the additional loss of m/z 59 during MS² fragmentation. MS³ fragmentation of the latter
222 fragment resulted in the apparent loss of another fatty acid which generated an m/z 116
223 product.

224 **HRAM/OT/MS analysis of unidentified IPL group III.** The lipid extract of *T.*
225 *sphagniphila* was subjected to HRAM/OT/MS analysis to elucidate the elemental
226 composition of the lipid head groups of the three unknown lipid clusters. Group III was the
227 most abundant IPL and therefore analyzed first. As was the case in IT/MS² fragmentation, the
228 initial loss observed for the molecular ion of m/z 665.5824 from group III, the apparently most
229 abundant unidentified IPL group in *T. sphagniphila*, is of a C16:1 fatty acid (Fig. 3A).
230 Subsequent loss of C₃H₉N generates m/z 352.2847, the base peak in the mass spectrum. The
231 presence of C₃H₉N, potentially a trimethylated nitrogen, is a common molecular feature in
232 other membrane lipid head groups such as PCs and betaines. From the base peak, a loss of a
233 C16:0 ketene, results in a product at m/z 116.0709 with a molecular composition of
234 C₅H₁₀O₂N. The observed fragmentation for group III molecular ion m/z 665.5824 appears to
235 represent an ornithine-like lipid that is trimethylated on the ϵ -nitrogen position (Fig. 3B).
236 This fragmentation pattern was observed for all molecular ions in group III lipids (Tables 2,
237 3). Proposed gas phase fragmentation includes the formation of a cyclic head group structure
238 after loss of a fatty acid, the trimethylated nitrogen, and β -OH fatty acid. This fragmentation
239 is similar to the formation of the cyclic m/z 115 diagnostic product, formed by loss of H₂O in
240 the head group, observed during MS fragmentation of ornithine lipids (36). In total there are

241 six main lipids in group III with different fatty acid compositions (m/z 693 consists of two co-
242 eluting isobaric lipids), which follow the proposed fragmentation pattern for the
243 trimethylornithine (TMO) structure (Tables 2, 3). Analysis by GC and GC/MS of the *T.*
244 *sphagniphila* extract confirmed that C18:1 ω 5c and C16:1 ω 5c fatty acids were the most
245 abundant core lipids, followed by C16:0, C18:0, β OH-C16, β OH-C18, and C17:0 fatty acids.
246 This is in agreement with previous lipid analysis reported by Kulichevskaya *et al.* (22).

247 **Structural identification of trimethylornithine lipids by NMR.** *T. sphagniphila*
248 group III lipids appeared to be the most abundant unknown lipid cluster among the four
249 analyzed planctomycetes. This lipid cluster was purified using semi-preparatory HPLC for
250 further analysis. In addition, ornithine lipids were purified from *F. johnsoniae* (Fig. 2) to be
251 used as a reference compound for structural comparison to the *T. sphagniphila* group III
252 lipids. Approximately 2 mg of group III lipid was isolated from the *T. sphagniphila* lipid
253 extract and 5 mg of ornithine lipid was isolated from *F. johnsoniae* lipid extract for NMR
254 analysis.

255 The $^1\text{H-NMR}$, COSY, and $^{13}\text{C-NMR}$ spectra of the purified ornithine lipid agreed well
256 with previously reported NMR structural characterization of ornithine lipids (37, 38). There
257 were many similarities between the $^1\text{H-NMR}$ and $^{13}\text{C-NMR}$ signals of the purified group III
258 lipids and ornithine lipids, particularly for the aliphatic chains (Table 4). The main
259 differences between the TMO lipid and ornithine $^1\text{H-NMR}$ spectra were the intense signal at
260 3.27 ppm in the TMO lipid spectra, the absence of a $\epsilon\text{-NH}_2$ signal at 5.71 ppm, and the
261 increase in chemical shift of the $\alpha\text{-NH}$ and head group δ -position signals. Both the $^1\text{H-NMR}$
262 and $^{13}\text{C-NMR}$ chemical shifts of the unknown signal (^1H 3.27 ppm, ^{13}C 54 ppm) and the head
263 group δ -position (^1H 3.70, ^{13}C 66 ppm) in the TMO lipids match with the chemical shifts of
264 the trimethylamine ($(\text{CH}_3)_3\text{N}^+$) group and adjacent carbon position (CH_2) reported for the
265 choline group of PC lipids in previous studies ($(\text{CH}_3)_3\text{N}^+$: ^1H 3.25, ^{13}C 54.2; CH_2 : ^1H 3.70, ^{13}C

266 66.1 – (39); (CH₃)₃N⁺: ¹³C 54.3; CH₂: ¹³C 66.65 – (40); (CH₃)₃N⁺: ¹H 3.30, ¹³C 54.6 – (41)).
267 (¹H, ¹³C)-Heteronuclear single quantum correlation spectroscopy (HSQC) analysis revealed
268 that the apparent trimethylamine proton at 3.27 ppm was directly bound to the carbon atom at
269 54 ppm. The (¹H, ¹³C)-HSQC analysis also showed that the head group δ-position ¹H
270 chemical shift was bound to an increased ¹³C-NMR chemical shift as well compared to the
271 head group δ-position signal in the ornithine lipid spectra.

272 Further confirmation of structural assignments was given by heteronuclear multiple
273 bond correlation spectroscopy (HMBC) which showed a connectivity between the apparent
274 trimethylamine signal and head group δ-position, and nuclear Overhauser effect spectroscopy
275 (NOESY), which confirmed a short distance between the trimethylamine signal and head
276 group δ-protons as well as the other head group and fatty acid chain protons. The presence of
277 a highly charged quaternary amine in the lipid head group explains the absence of the δ-NH₂
278 signal in the proton spectrum, since no protons are attached directly to the nitrogen. It may
279 also be expected that that this functional group increases the chemical shift of the α-NH
280 compared to the ornithine lipid as observed. Alkene chemical shifts in the TMO NMR
281 spectra (Table 4) were expected to be detected, as observed in the MS results. Therefore, the
282 NMR results confirm the structural identification of the lipids in group III as a series of
283 ornithine lipids that are trimethylated on the ε-nitrogen position (Fig. 3B, Table 2, 3, 4).

284 **Structural elucidation of IPL groups II and I.** The HRAM/OT/MS fragmentation of
285 *T. sphagniphila* group II molecular ion *m/z* 651.5666 and group I *m/z* 637.5519 produced the
286 same initial losses of a C16:1 fatty acid as observed for the TMO *m/z* 665.5824 lipid (Figs. 4,
287 5; Table 2). The thus formed group II *m/z* 379.3429 ion then loses C₂H₇N, while group I
288 formed *m/z* 383.3429 loses CH₅N (Figs. 4, 5, Table 3). Analogues to the loss of C₃H₉N for
289 trimethylornithine, the loss of C₂H₇N and CH₅N appears to indicate dimethylated and
290 monomethylated nitrogen structures, respectively (Figs. 4, 5). After the methylated nitrogen

291 losses, the formed m/z 352.2847 ions for both group II m/z 651.5666 and group I m/z
292 637.5519 lose a C16:0 fatty acid, identical to what has been observed for the TMOs (Table 2),
293 resulting in the same m/z 116.0710 C₅H₁₀NO₂ product (Table 3; Figs. 4, 5). For group II,
294 fragmentation also resulted in formation of m/z 144.1021, m/z 161.1285, and m/z 187.1079
295 ions, and for group I, fragmentation resulted in m/z 129.1024, m/z 147.1129, and m/z
296 173.0921 products (Table 3, Fig. 4, 5). These fragmentation patterns were the same for all
297 group II and group I lipids, respectively (Table 2).

298 Based on the fragmentation behavior and formula assignments of key losses and
299 products we propose that the unknown lipids in cluster II represent a series of ornithine lipids
300 that are dimethylated on the ϵ -nitrogen position, i.e. dimethylornithine (DMO, Fig. 4B), while
301 unknown lipids in cluster I represent ornithine lipids that are monomethylated on the ϵ -
302 nitrogen position, i.e. monomethylornithine (MMO, Fig. 5B). As with the TMO cluster, there
303 were five main masses in both the DMO and MMO clusters that represent six lipids (Tables 2,
304 3). The fatty acid distribution was identical among the MMO, DMO, and TMO lipid groups
305 and the relative abundance of the various lipids within each group was similar (Table 2).
306 Under the chromatographic conditions used here, the elution order of ornithine, MMO, DMO,
307 and TMO was the same as observed for PE, MMPE, DMPE, and PC lipids identified in the
308 *Gemmata*-like SP5 lipid extract (Fig 2D), displaying an increasing retention time with
309 increasing methylation of the ϵ -nitrogen.

310 **Distribution of MMO, DMO, and TMO lipids in planctomycete strains.** The
311 trimethylornithine lipids appeared to be the most abundant of the three classes of
312 methylornithines in each of the four planctomycetes (Fig 2). The MMO, and DMO lipids
313 were both most abundant in *T. sphagniphila*, followed by *Gemmata*-like strain SP5, *S. rosea*,
314 and *S. acidiphila*. The dominant core lipids observed in MMO, DMO, and TMOs were C18:1
315 and C16:1 for *T. sphagniphila*, C18:1 and C18:0 for *S. rosea*, C18:1, C18:0 for *S. acidiphila*,

316 and C20:1 and C16:0 for the *Gemmata*-like strain SP5. This difference in fatty acid
317 distribution observed between the lipid extracts of the four planctomycete species based on
318 HPLC/ESI/IT/MS fragmentation among the MMO, DMO, and TMO lipids resulted in slightly
319 different retention times of the three lipid classes for each species in the base peak
320 chromatograms (Fig 2).

DISCUSSION

321
322 This study describes the identification of a series of novel OLs with increasing
323 methylation on the terminal ϵ -nitrogen position, resulting in mono-, di- and trimethylated
324 ornithine head groups. OLs are common phosphorus-free membrane lipids in bacteria, but
325 absent in Eukaryotes and Archaea (42-43). Roughly 25% of bacteria whose genomes have
326 been sequenced have the predicted capability to produce OLs (44). It has been proposed that
327 OLs are important for outer membrane stability in Gram-negative bacteria due to their
328 zwitterionic nature (45). In some bacteria OLs are produced under phosphorus limitation (46-
329 47), or hydroxylated under thermal or acid stress (48-50). Other amino acid-containing lipids
330 have been identified in various bacteria including glycine lipids (51-52), a lysine lipid (53),
331 and an ornithine-aurine linked lipid (54), although they are not nearly as widespread as OLs.
332 While the exact function of OL modifications is not yet fully described, characterization of
333 mutants that are deficient in ornithine lipid biosynthesis and modification genes has further
334 supported a mechanism of bacterial stress response to changing environmental conditions (44,
335 49-50). The unique environmental settings from which the planctomycetes in this study were
336 isolated, and the adaptable nature of ornithine lipids in various bacteria, suggest that the
337 synthesis of methylated ornithine lipids by these microbes may be a response to the
338 ombrotrophic conditions of northern wetlands.

339 Increasing acidity ultimately impedes microorganism growth, causing a range of
340 physiological problems, including outer membrane damage (55). Various microbes have
341 developed different strategies to respond to pH stress (56-58). The hydroxylation of ornithine
342 lipids in *Rhizobium tropici* under acidic conditions increases the potential for hydrogen
343 bonding among individual polar lipid molecules resulting in greater membrane stability (49-
344 50). Like PEs, MMPEs, DMPEs, and PCs, the addition of each subsequent methyl group to
345 the ϵ -NH₂ ornithine head group in MMOs, DMOs, and TMOs appears to increase the polarity

346 of the lipid based on LC retention time. This is especially true in the TMO lipids where the
347 presence of a quaternary amine yields a charged choline-like moiety similar to that of PCs.
348 Due to their polarity and relatively cylindrical shape, PCs spontaneously form bilayers,
349 whereas the cone shape of PEs (non-methylated equivalent to PC) causes it to assemble into
350 inverted hexagonal phases. Perhaps, the additional three methyl groups in the head group of
351 TMO also give it a more cylindrical shape and greater polarity compared to non-modified
352 ornithine lipids, and thus result in greater bilayer stability. The ombrotrophic wetlands, where
353 these planctomycetes were isolated from, are acidic and nutrient-poor ecosystems, and all the
354 four species in which the TMO lipid were observed are moderately acidophilic (19, 21-22).
355 Increased membrane stability provided by a polar quaternary amine in lipid head groups
356 would be beneficial to these organisms in their native environment. Furthermore, because
357 these ecosystems are nutrient limited, the synthesis of TMO lipids could provide membrane
358 stability without relying on limited phosphorus. It has been shown that marine microbes in
359 phosphorus limited conditions will switch from producing phosphorus containing membrane
360 lipids such as PCs and PGs to non-phosphorus containing lipids such as betaines and
361 sulfoquinovosyl diacylglycerols (SQDGs) to maintain growth and survival (59). We
362 hypothesize that the increased polarity and possible cylindrical shape of the trimethylornithine
363 head group provides membrane stability without using scarce phosphorus and is thus, an
364 adaptation to the acidic, nutrient-poor conditions of *Sphagnum*-dominated European North
365 Russian wetlands.

366 The distributions of core lipid chains among MMO, DMO, TMO lipids in *T.*
367 *sphagniphila* are identical among the three lipid classes (Table 2). There are also many
368 similarities in core lipid distribution among MMO, DMO, and TMO lipids within the extracts
369 of *S. rosea*, *S. acidiphila*, and *Gemmata*-like strain SP5. The similar fatty acid distribution
370 among the three lipid classes within each species suggests a biosynthetic link between these

371 classes. This sequence of lipids with increasing methylation is not unprecedented in
372 membrane lipids. One of the pathways for biosynthesis of PC involves sequential
373 methylation of PE by the enzyme phosphatidylethanolamine N-methyltransferase producing
374 MMPE and DMPE as intermediates (60-62). A similar methylation process of the ornithine
375 lipid head group may be involved in the biosynthesis of methylornithine lipids.

376 Pyrosequencing of bacterial 16S rRNA gene fragments was performed by
377 Kulichevskaya *et al.* (22) for the peat sample from which *T. sphagniphila* was originally
378 isolated in order to assess importance of this species to the *Planctomycete* community. The
379 study revealed that *T. sphagniphila* accounted for 10% of the planctomycete-related reads
380 obtained from the peat sample, therefore suggesting that *T. sphagniphila* is a typical
381 representative of *Planctomyces* in peat bogs (22). *Singulisphaera*-like planctomyces were
382 also abundant in this peat sample. However, the majority (61%) of all planctomycete-related
383 16S rRNA gene sequences retrieved from this sample could not be assigned to taxonomically
384 described organisms, leaving open the possibility that other species at this location produce
385 TMO lipids as well. *Planctomyces* have been observed to account for up to 14% of total
386 bacterial cells in the upper, oxic peat layers of acidic northern wetlands and were mostly
387 represented by members of the *Isosphaera-Singulisphaera* group (17). This suggests that the
388 TMOs may be an important membrane constituent among the *Planctomycete* community in
389 peat bogs, and may serve as an important environmental adaptation towards this group's
390 function as slow acting decomposers of plant-derived organic matter. Further research is
391 needed to investigate the specific function of these lipids, the mono-, di-, and trimethylated
392 ornithine lipid biosynthetic pathway, and the importance of methylornithine lipids in
393 ombrotrophic environments.

394

REFERENCES

- 395 1. **Kivinen E, and Pakarinen P.** 1991. Geographical Distribution of Peat Resources and Major
396 Peatland Complex Types in the World, *Ann. Acad. Scient. Fenn.-math.* **A3**:132:1-28.
- 397 2. **Gorham E.** 1991. Northern Peatlands: Role in Carbon Cycle and Probable Responses to Climate
398 Warming. *Ecol. Appl.* **1**:182-195.
- 399 3. **Bain CG, Bonn A, Stoneman R, Chapman S, Coupar A, Evans M, Gearey B, Howat M, Joosten**
400 **H, Keenleyside C, Labadz J, Lindsay R, Littlewood N, Lunt P, Miller CJ, Moxey A, Orr H, Reed**
401 **M, Smith P, Swales V, Thompson DBA, Thompson PS, Van de Noort R, Wilson JD, and Worrall**
402 **F.** 2011. IUCN UK Commission of Inquiry on Peatlands. IUCN UK Peatland Programme, Edinburgh.
- 403 4. **Gajewski K, Viau A, Sawada M, Atkinson D, and Wilson S.** 2001. *Sphagnum* peatland distribution
404 in North America and Eurasia during the past 21,000 years. *Glob. Biogeochem. Cyc.* **15**:297-310.
- 405 5. **Clymo RS.** 1965. Experiments on breakdown of *Sphagnum* in two bogs. *J. Ecol.* **53**:747-758.
- 406 6. **Coulson JC, and Butterfield J.** 1978. An investigation of the biotic factors determining the rates of
407 plant decomposition on blanket bog. *J. Ecol.* **66**:631-650.
- 408 7. **Johnson LC, and Damman AWH.** 1993. Decay and its regulation in *Sphagnum* peatlands. *Adv. Bryol.*
409 **5**:249-296.
- 410 8. **Verhoeven JTA, and Liefveld WM.** 1997. The ecological significance of organochemical compounds
411 in *Sphagnum*. *Acta Bot. Neerl.* **46**:117-130.
- 412 9. **Aerts R, Wallén B, Malmer N, and de Caluwe H.** 2001. Nutritional constraints on *Sphagnum*-growth
413 and potential decay in northern peatlands. *J. Ecol.* **89**:292-299.
- 414 10. **Moore PD, and Bellamy DJ.** 1974. Peatlands. London, UK: Elek. Science 221 pp.
- 415 11. **Clymo RS.** 1984. The limits to peat bog growth. *Philos. Trans. R. Soc. Lond. B. Biol. Sci.* **303**:605-654.
- 416 12. **Botch MS, Kobak KI, Vinson TS, and Kolchugina TP.** 1995. Carbon pools and accumulation in
417 peatlands of the former Soviet Union. *Glob. Biogeochem. Cyc.* **9**:37-46.
- 418 13. **Dedysh SN, Pankratov TA, Belova SE, Kulichevskaya IS, and Liesack W.** 2006. Phylogenetic
419 analysis and in situ identification of *Bacteria* community composition in an acidic *Sphagnum* peat bog.
420 *Appl. Env. Microbiol.* **72**:2110-2117.
- 421 14. **Kulichevskaya IS, Belova SE, Kevbrin VV, Dedysh SN, and Zavarzin GA.** 2007a. Analysis of the
422 bacterial community developing in the course of the *Sphagnum* moss decomposition. *Microbiol.*
423 **76**:621-629.
- 424 15. **Pankratov TA, Ivanova AO, Dedysh SN, and Liesack W.** 2011. Bacterial populations and
425 environmental factors controlling cellulose degradation in an acidic *Sphagnum* peat. *Env. Microbiol.*
426 **13**:1800-1814.
- 427 16. **Kulichevskaya IS, Pankratov TA, and Dedysh SN.** 2006. Detection of representatives of the
428 *Planctomycetes* in *Sphagnum* peat bogs by molecular and cultivation approaches. *Microbiol.* **75**:389-
429 396.
- 430 17. **Ivanova AO, and Dedysh SN.** 2012. Abundance, diversity, and depth distribution of *Planctomycetes* in
431 acidic northern wetlands. *Front. Microbiol.* **3**:5.
- 432 18. **Kulichevskaya IS, Ivanova AO, Belova SE, Baulina OI, Bodelier PLE, Rijpstra WIC, Sinninghe**
433 **Damsté JS, Zavarzin GA, and Dedysh SN.** 2007b. *Schlesneria paludicola* gen. nov., sp. nov., the first
434 acidophilic member of the order *Planctomycetes* from *Sphagnum*-dominated boreal wetlands. *Int. J.*
435 *Syst. Evol. Microbiol.* **57**:2680-2687.

- 436 19. **Kulichevskaya IS, Ivanova AO, Baulina OI, Bodelier PLE, Sinninghe Damsté JS, and Dedysh SN.**
437 2008. *Singulisphaera acidiphila* gen. nov., sp. nov., a non-filamentous, *Isosphaera*-like planctomycete
438 from acidic northern wetlands. *Int. J. Syst. Evol. Microbiol.* **58**:1186-1193.
- 439 20. **Kulichevskaya IS, Baulina OI, Bodelier PLE, Rijpstra WIC, Sinninghe Damsté JS, and Dedysh**
440 **SN.** 2009. *Zavarzinella formosa* gen. nov., sp. nov., a novel stalked, *Gemmata*-like planctomycete from
441 a Siberian peat bog. *Int. J. Syst. Evol. Microbiol.* **59**:357-364.
- 442 21. **Kulichevskaya IS, Detkova EN, Bodelier PLE, Rijpstra WIC, Sinninghe Damsté JS, and Dedysh**
443 **SN.** 2012a. *Singulisphaera rosea*, sp. nov., a planctomycete from *Sphagnum* Peat, and emended
444 description of the genus *Singulisphaera*. *Int. J. Syst. Evol. Microbiol.* **62**:118-123.
- 445 22. **Kulichevskaya IS, Serkebaeva YM, Kim Y, Rijpstra WIC, Sinninghe Damsté JS, Liesack W, and**
446 **Dedysh SN.** 2012b. *Telmatocola sphagniphila* gen. nov., sp. nov., a novel dendriform planctomycete
447 from northern wetlands. *Front. in Microbiol.* **3**:146.
- 448 23. **St-Hilaire F, Wu J, Roulet NT, Folking S, Lafleur PM, Humphreys ER, and Arora V.** 2010.
449 McGill wetland model: evaluation of a peatland carbon simulator developed for global assessments.
450 *Biogeosci.* **7**:3517-3530.
- 451 24. **Wu J, Roulet NT, Nilsson M, Lafleur P, and Humphreys E.** 2012. Simulating the carbon cycling of
452 northern peatlands using a land surface scheme coupled to a wetland carbon model. *Atm. Oc.* **50**: 487-
453 506.
- 454 25. **Kirschbaum MUF.** 1995. The temperature dependence of soil organic matter decomposition, and the
455 effect of global warming on soil organic C storage. *Soil Biol. Biochem.* **27**:753-760.
- 456 26. **Biasi C, Rusalimova O, Meyer H, Kaiser C, Wanek W, Barsukov P, Junger H, Richter A.** 2005.
457 Temperature-dependent shift from labile to recalcitrant carbon sources of arctic heterotrophs. *Rapid*
458 *Commun. Mass Spectrom.* **19**:1401-1408.
- 459 27. **Dorrepaal E, Toet S, van Logtestijn RSP, Swart E, van de Weg MJ, Callaghan TV, and Aerts R.**
460 2009. Carbon respiration from subsurface peat accelerated by climate warming in the subarctic. *Nature*
461 **460**:616-620.
- 462 28. **Sturt HF, Summons RE, Smith K, Elvert M, and Hinrichs KU.** 2004. Intact polar membrane lipids
463 in prokaryotes and sediments deciphered by high-performance liquid chromatography/electrospray
464 ionization multistage mass spectrometry—new biomarkers for biogeochemistry and microbial ecology.
465 *Rap. Commun. Mass Spectrom.* **18**:617-628.
- 466 29. **Schubotz F, Wakeham SG, Lipp JS, Fredericks HF, Hinrichs KU.** 2009. Detection of microbial
467 biomass by intact polar membrane lipid analysis in the water column and surface sediments of the Black
468 Sea. *Environm. Microbiol.* **11**:2720-2734.
- 469 30. **Staley JT, Fuerst JA, Giovannoni S, and Schlesner H.** 1992. The order *Planctomycetales* and the
470 genera *Planctomyces*, *Pirellula*, *Gemmata* and *Isosphaera*. In *The Prokaryotes: a Handbook on the*
471 *Biology of Bacteria: Ecophysiology, Isolation, Identification, Applications*, 2nd edn. Pp. 3710-3731.
472 Edited by A. Balows, H. Truper, M. Dworkin, W. Harder & K.H. Schleifer. NewYork: Springer.
- 473 31. **Rütters H, Sass H, Cypionka H, and Rullkötter J.** 2002. Phospholipid analysis as a tool to study
474 complex microbial communities in marine sediments. *J. Microbiol. Meth.* **48**:149-160.
- 475 32. **Sinninghe Damsté JS, Rijpstra WIC, Hopmans EC, Weijers JWH, Foessel BU, Overmann J, and**
476 **Dedysh SN.** 2011. 13,16-Dimethyl octacosanedioic acid (iso-diabolic acid), a common membrane-
477 spanning lipid of *Acidobacteria* subdivisions 1 and 3. *Appl. Env. Microbiol.* **77**:4147-4154.
- 478 33. **Sinninghe Damsté JS, Rijpstra, WIC, Schouten S, Fuerst JA, Jetten MSM, and Strous M.** 2004.
479 The occurrence of hopanoids in planctomycetes: implications for the sedimentary biomarker record.
480 *Org. Geochem.* **35**:561-566.

- 481 34. **Boumann HA, Longo ML, Stroeve P, Poolman B, Hopmans EC, Stuart MCA, Sinninghe Damsté**
482 **JS, Schouten S.** 2009. Biophysical properties of membrane lipids of anammox bacteria: I. Ladderane
483 phospholipids form highly organized fluid membranes. *Biochim. Biophys. Acta* **1788**: 1444-1451.
- 484 35. **Smittenberg RH, Hopmans EC, Schouten S, Sinninghe Damsté JS.** 2002. Rapid isolation of
485 biomarkers for compound specific radiocarbon dating using high performance liquid chromatography
486 and flow injection analysis-atmospheric pressure chemical ionisation mass spectrometry. *J. Chromatogr.*
487 *A* **978**:129-140.
- 488 36. **Zhang X, Ferguson-Miller SM, and Reid GE.** 2009. Characterization of ornithine and glutamine
489 lipids extracted from cell membranes of *Rhodobacter sphaeroides*. *J. ASMS* **20**:198-212.
- 490 37. **Okuyama H, and Monde K.** 1996. Identification of an ornithine-containing lipid from *Cytophaga*
491 *johnsonae* Stanier strain C21 by ¹H-NMR. *Chem. and Phys. Lipids*. **83**:169-173.
- 492 38. **Linscheid M, Diehl BWK, Overmohle M, Riedl I, and Heinz E.** 1997. Membrane lipids of
493 *Rhodospseudomonas viridis*. *Biochim. et Biophys. Acta – Lipids and Lipid Metabol.* **1347**:151-163.
- 494 39. **Hamilton JA, and Morrisett JD.** 1986. Nuclear magnetic resonance studies of lipoproteins. *Meth.*
495 *Enzymol.* **128**:472-515.
- 496 40. **Gunstone FD.** 1994. High resolution ¹³C NMR. A technique for the study of lipid structure and
497 composition. *Prog. Lipid Res.* **33**:19-28.
- 498 41. **Tugnoli V, Bottura G, Fini G, Reggiani A, Tinti A, Trincherio A, and Tosi MR.** 2003. ¹H-NMR and
499 ¹³C-NMR lipid profiles of human renal tissues. *Biopolym.* **72**:86-95.
- 500 42. **Lopez-Lara IM, Sohlenkamp C, and Geiger O.** 2003. Membrane lipids in plant-associated bacteria:
501 their biosynthesis and possible functions. *Molec. Plant-Microb. Int.* **16**:567-579.
- 502 43. **Geiger O, Gonzalez-Silva N, Lopez-Lara IM, and Sohlenkamp C.** 2010. Amino acid-containing
503 membrane lipids in bacteria. *Prog. Lipid Res.* **49**:46-60.
- 504 44. **Vences-Guzman MA, Geiger O, and Sohlenkamp C.** 2012. Ornithine lipids and their structural
505 modifications from A to E and beyond. *FEMS Microbiol. Letters* **335**:1-10.
- 506 45. **Freer E, Moreno E, Moriyon I, Pizarro-Cerda J, Weintraub A, and Gorvel JP.** 1996. *Brucella-*
507 *Salmonella* lipopolysaccharide chimeras are less permeable to hydrophobic probes and more sensitive to
508 cationic peptides and EDTA than are their native *Brucella sp* counterparts. *J. Bacteriol.* **178**:5867-5876.
- 509 46. **Weissenmayer B, Gao JL, Lopez-Lara IM, and Geiger O.** 2002. Identification of a gene required for
510 the biosynthesis of ornithine-derived lipids. *Molec. Microbiol.* **45**:721-733.
- 511 47. **Gao JL, Weissenmayer B, Taylor AM, Thomas-Oates J, Lopez-Lara IM, and Geiger O.** 2004.
512 Identification of a gene required for the formation of lyso-ornithine lipid, an intermediate in the
513 biosynthesis of ornithine-containing lipids. *Molec. Microbiol.* **53**:1757-1770.
- 514 48. **Taylor CJ, Anderson AJ, and Wilkinson SG.** 1998. Phenotypic variation of lipid composition in
515 *Burkholderia cepacia*: a response to increased growth temperature is a greater content of 2-hydroxy
516 acids in phosphatidylethanolamine and ornithine amide lipid. *Microbiol.* **144**:1737-45.
- 517 49. **Rojas-Jimenez K, Sohlenkamp C, Geiger O, Martinez-Romero E, Werner D, and Vinuesa**
518 **P.** 2005. A ClC chloride channel homolog and ornithine-containing membrane lipids of *Rhizobium*
519 *tropicum* CIAT899 are involved in symbiotic efficiency and acid tolerance. *Molec. Plant-Microbe Int.*
520 **18**:1175-1185.
- 521 50. **Vences-Guzman MA, Guan Z, Ormeno-Orillo E, Gonzalez-Silva N, Geiger O, and Sohlenkamp C.**
522 2011. Hydroxylated ornithine lipids increase stress tolerance in *Rhizobium tropicum* CIAT899. *Molec.*
523 *Biol.* **79**:1496-1514.

- 524 51. **Kawazoe R, Okuyama H, Reichardt W, and Sasaki S.** 1991. Phospholipids and a novel glycine
525 containing lipoamino acid in *Cytophaga johnsonae* stainier strain C21. J. Bacteriol. **173**:5470-5475.
- 526 52. **Batrakov SG, Nikitin DI, Mosezhnyi AE, and Ruzhitsky AO.** 1999. A glycine containing
527 phosphorus-free lipoaminoacid from the gram-negative marine bacterium *Cyclobacterium marinus* WH.
528 Chem. Phys. Lipids **99**:139-143.
- 529 53. **Tahara Y, Yamada Y, and Kondo K.** 1976a. A new lysine-containing lipid isolated from
530 *Agrobacterium tumefaciens*. Agric. Biol. Chem. **40**:1449-1450.
- 531 54. **Tahara Y, Kameda M, Yamada Y, and Kondo K.** 1976b. A new lipid; the ornithine and taurine-
532 containing "cerilipin". Agric. Biol. Chem. **40**:243-244.
- 533 55. **Brown JL, Ross T, McMeekin TA, and Nichols PD.** 1997. Acidic habituation of *Escherichia coli* and
534 the potential role of cyclopropane fatty acids in low pH tolerance. Int. J. Food Microbiol. **37**:163-173.
- 535 56. **Bearson S, Bearson B, and Foster JW.** 1997. Acidic stress responses in enterbacteria- minireview.
536 FEMS Microbiol. Lett. **147**:173-180.
- 537 57. **Álvarez-Ordóñ A, Fernández A, López M, and Bernardo A.** 2008. Relationship between membrane
538 fatty acid composition and heat resistance of acid and cold stressed *Salmonella senftenberg* CECT 4348.
539 Food Microbiol. **26**:347-353.
- 540 58. **Gianotti A, Iucci L, Guerzoni ME, and Lanciotti R.** 2009. Effect of acidic conditions on fatty acid
541 composition and membrane fluidity of *Escherichia coli* strains isolated from Crescenza cheese. Annal.
542 Microbiol. **59**:603-610.
- 543 59. **Van Mooy BAS, Fredericks HF, Pedler BE, Dyhrman ST, Karl DM, Koblizek M, Lomas MW,**
544 **Mincer TJ, Moore LR, Moutin T, Rappé MS, and Webb EA.** 2009. Phytoplankton in the ocean use
545 non-phosphorus lipids in response to phosphorus scarcity. Nature **458**:69-72.
- 546 60. **Bremer J, and Greenberg DM.** 1961. Methyl transferring enzyme system of microsomes in
547 biosynthesis of lecithin (phosphatidylcholine). Biochim. Biophys. Acta **46**:205-216.
- 548 61. **Yamashita S, Oshima A, Nikawa J, and Hosaka K.** 1982. Regulation of the
549 phosphatidylethanolamine methylation pathway in *Saccharomyces cerevisiae*. Eur. J. Biochem.
550 **128**:589-595.
- 551 62. **Gaynor PM, Gill T, Toutenhoofd S, Summers EF, McGraw P, Homann MJ, Henry SA, and**
552 **Carman GM.** 1991. Regulation of phosphatidylethanolamine methyltransferase and phospholipid
553 methyltransferase by phospholipid precursors in *Saccharomyces cerevisiae*. Biochim. Biophys. Acta
554 **1090**:326-332.

555

TABLES

556 **Table 1:** Contribution of group I, II and III lipids (%) to the total lipid signal as determined
 557 from the ESI/IT/MS base peak chromatogram of *T. sphagniphila*, *S. rosea*, *S. acidiphila*, and
 558 *Gemmata*-like SP5 strain lipid extracts.

	I	II	III
<i>T. sphagniphila</i>	24.7	13.9	45.3
<i>S. rosea</i>	<1.0	3.6	44.4
<i>S. acidiphila</i>	<1.0	<1.0	37.2
SP5	<1.0	4.8	49.9

559 **Table 2:** The m/z of the molecular species, fatty acid losses, elemental composition, and
 560 accuracy values (Δ mmu**) that occur during MS fragmentation of each mass in lipid groups
 561 III (TMO), II (DMO), and I (MMO). R2-COOH and R1-CH=C=C=O losses result from
 562 fragmentation to fatty acid (FA) and β OH-fatty acid (β OH-FA) respectively in the structure
 563 below. For TMO: R3 = R4 = R5 = CH₃; DMO: R3 = R4 = CH₃, R5 = H; MMO: R3 = CH₃,
 564 R4 = R5 = H.

565 *Relative abundance (Rel. Abun.) indicates the peak area percentage of each lipid within its
 566 respective group.

567 **In general the 0.5 Δ mmu (milli mass unit) range was used as a measure of very high
 568 confidence molecular formula assignments and the 1.0 Δ mmu range was used as a measure
 569 of good confidence molecular formula assignments (Kostiainen et al., 1997; Sakayanagi et al.,
 570 2006; Calza et al., 2012).

571 **Table 3:** The m/z , HRAM/OT/MS assigned molecular formulas, elemental composition, and
 572 accuracy values (Δ mmu) of formula assignments of observed losses and products that occur
 573 during MS fragmentation (Figure 2, 3, 4) of each mass in lipid groups III (TMO), II (DMO),
 574 and I (MMO). Elemental composition shown below Δ mmu values.

575 **Table 4:** ^{13}C - and ^1H -NMR signals (ppm) from trimethylornithine (structure below) and
576 ornithine lipids. Positions are shown below.

FIGURE LEGENDS

577

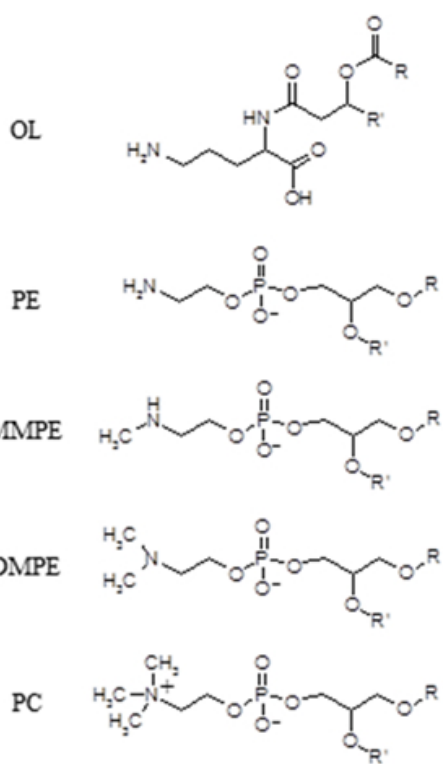
578 **Figure 1:** Molecular structures of ornithine lipid (OL); phosphatidylethanolamine (PE);
579 monomethylphosphatidylethanolamine (MMPE); dimethylphosphatidylethanolamine
580 (DMPE); phosphatidylcholine (PC).

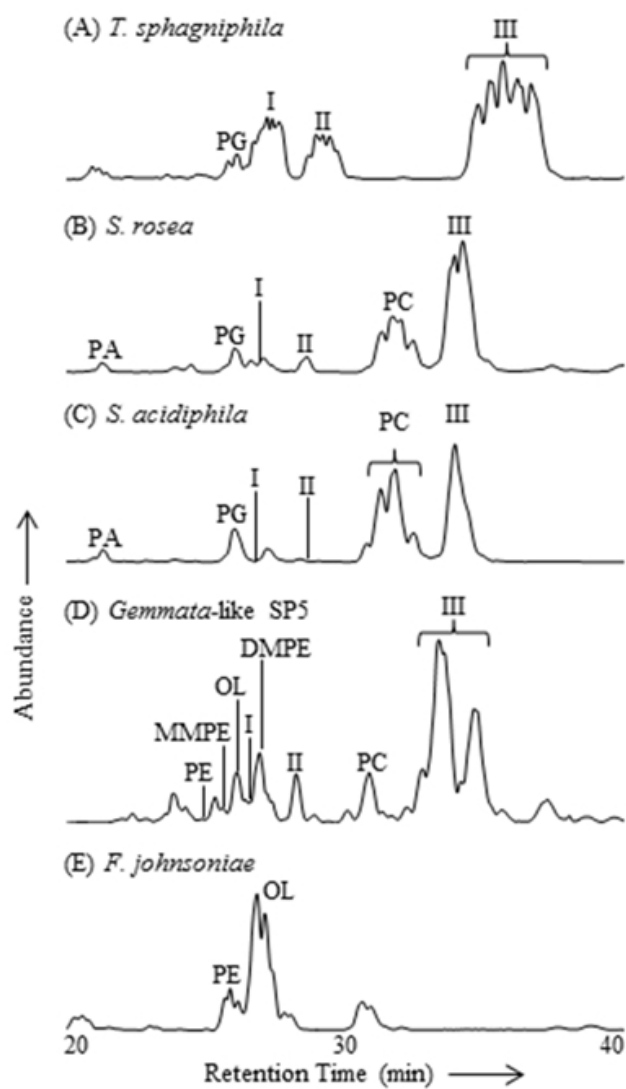
581 **Figure 2:** HPLC-ESI/IT/MS Ion Trap MS¹ base peak chromatograms (*m/z* 400-2000) of
582 Bligh & Dyer lipid extracts from planctomycete cultures: (A) *T. sphagniphila*; (B) *S. rosea*;
583 (C) *S. acidiphila*; (D) *Gemmata*-like SP5 strain; (E) *F. johnsoniae* (bacteriodete). PG =
584 phosphatidylglycerol; PA = phosphatidic acid; PC = phosphatidylcholine; PE =
585 phosphatidylethanolamine; MMPE = monomethylphosphatidylethanolamine; DMPE =
586 dimethylphosphatidylethanolamine; OL = ornithine lipid.

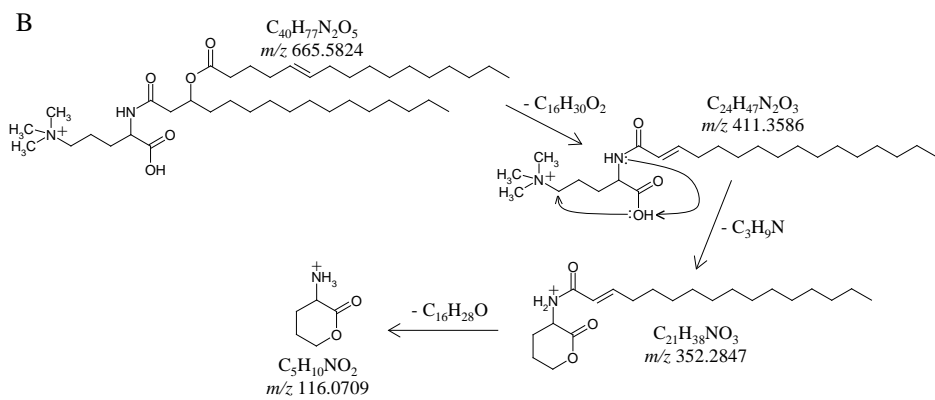
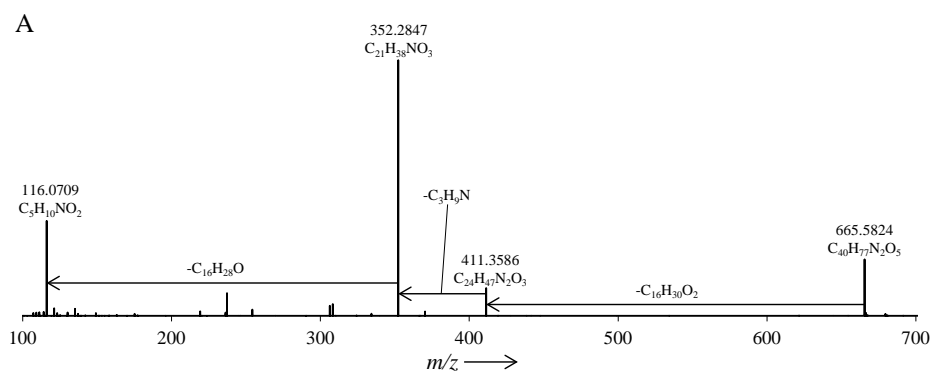
587 **Figure 3:** (A) High resolution accurate mass quadrupole OT MS² mass spectrum of *T.*
588 *sphagniphila* lipid extract group III trimethylornithine *m/z* 665.5824 (TMO: C16:1/C16:0).
589 Chemical formulas represent neutral losses and products after MS² fragmentation. (B)
590 Proposed gas-phase fragmentation pathway of trimethylornithine *m/z* 665.5824.

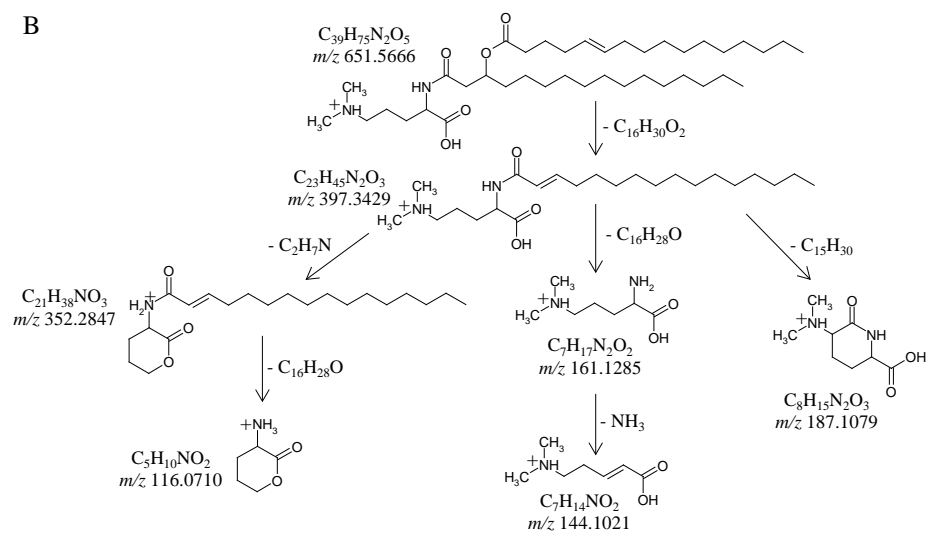
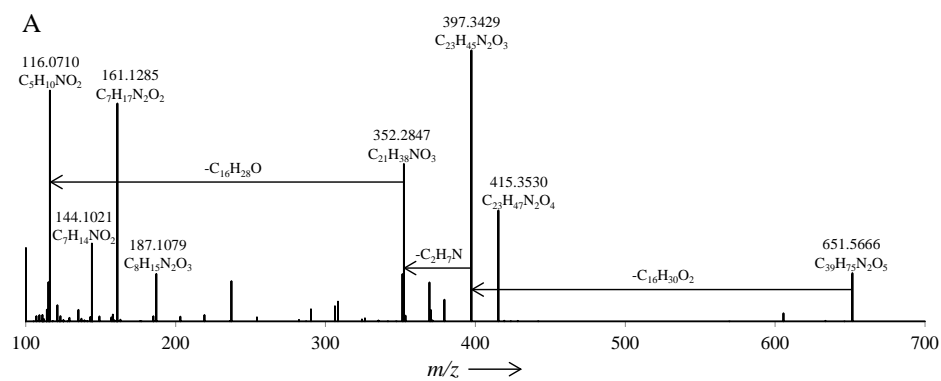
591 **Figure 4:** (A) High resolution accurate mass quadrupole OT MS² mass spectrum of *T.*
592 *sphagniphila* lipid extract group II dimethylornithine *m/z* 651.5666. Chemical formulas
593 represent neutral losses and products after MS² fragmentation. (B) Proposed gas-phase
594 fragmentation pathway of dimethylornithine *m/z* 651.5666.

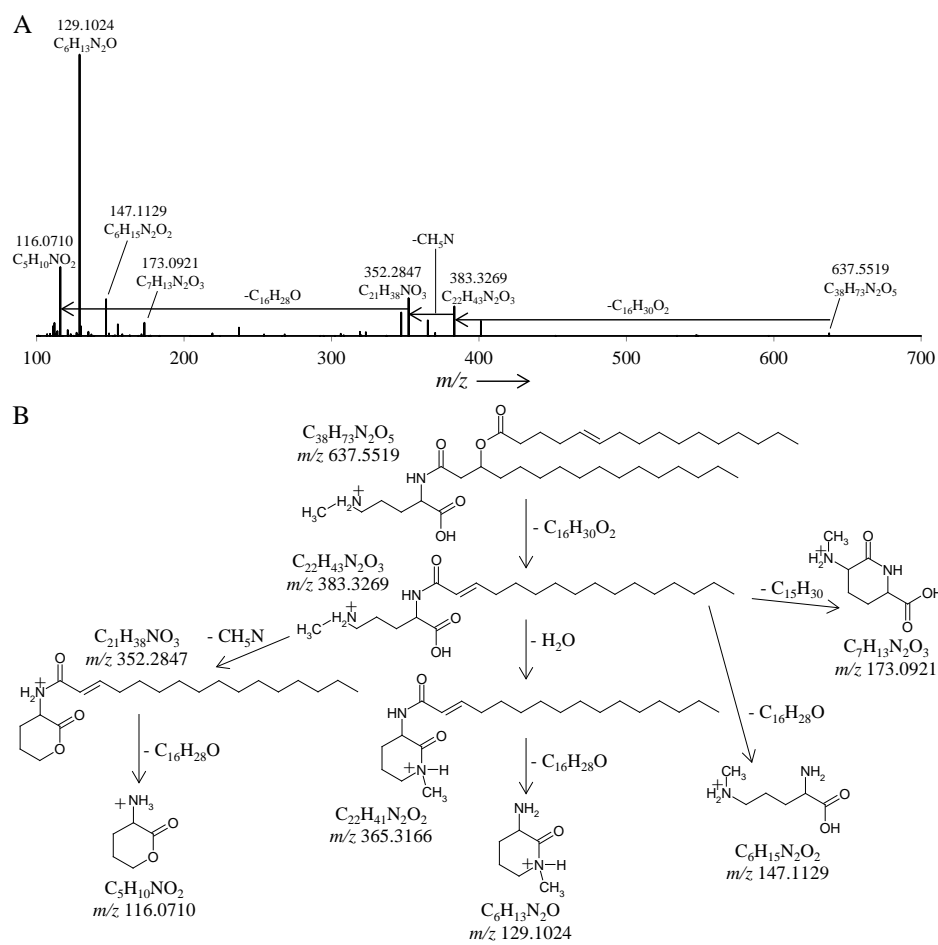
595 **Figure 5:** (A) High resolution accurate mass quadrupole OT MS² mass spectrum of *T.*
596 *sphagniphila* lipid extract group I monomethylornithine *m/z* 637.5519. Chemical formulas
597 represent neutral losses and products after MS² fragmentation. (B) Proposed gas-phase
598 fragmentation pathway of monomethylornithine *m/z* 637.5519.

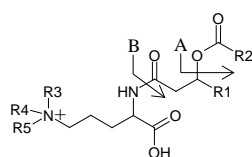




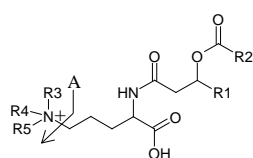




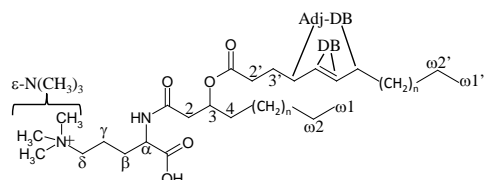




III (TMO)	M ⁺	Rel. Abun.* (%)	FA	^A Observed Loss R2-COOH	Assigned Elemental Composition	Δ mmu**	β OH-FA	^B Observed Loss R1-CH=C=C=O	Assigned Elemental Composition	Δ mmu**
C ₄₀ H ₇₇ N ₂ O ₅	665	20.4	C16:1	254.2239	C ₁₆ H ₃₀ O ₂	0.7	C16:0	236.2138	C ₁₆ H ₂₈ O	0.2
C ₄₁ H ₇₉ N ₂ O ₅	679	29.3	C16:1	254.2243	C ₁₆ H ₃₀ O ₂	0.3	C17:0	250.2291	C ₁₇ H ₃₀ O	0.6
C ₄₂ H ₈₁ N ₂ O ₅	693	7.3	C16:1	254.2252	C ₁₆ H ₃₀ O ₂	0.6	C18:0	264.2449	C ₁₈ H ₃₂ O	0.4
C ₄₂ H ₈₁ N ₂ O ₅	693	9.8	C18:1	282.2556	C ₁₈ H ₃₄ O ₂	0.3	C16:0	236.2137	C ₁₆ H ₂₈ O	0.3
C ₄₃ H ₈₃ N ₂ O ₅	707	23.8	C18:1	282.2556	C ₁₈ H ₃₄ O ₂	0.3	C17:0	250.2293	C ₁₇ H ₃₀ O	0.4
C ₄₄ H ₈₅ N ₂ O ₅	721	9.6	C18:1	282.2556	C ₁₈ H ₃₄ O ₂	0.3	C18:0	264.2447	C ₁₈ H ₃₂ O	0.6
II (DMO) [M+H] ⁺										
C ₃₉ H ₇₅ N ₂ O ₅	651	12.1	C16:1	254.2237	C ₁₆ H ₃₀ O ₂	0.9	C16:0	236.2137	C ₁₆ H ₂₈ O	0.3
C ₄₀ H ₇₇ N ₂ O ₅	665	27.2	C16:1	254.2251	C ₁₆ H ₃₀ O ₂	0.5	C17:0	250.2290	C ₁₇ H ₃₀ O	0.7
C ₄₁ H ₇₉ N ₂ O ₅	679	6.5	C16:1	254.2244	C ₁₆ H ₃₀ O ₂	0.2	C18:0	264.2446	C ₁₈ H ₃₂ O	0.7
C ₄₁ H ₇₉ N ₂ O ₅	679	14.2	C18:1	282.2554	C ₁₈ H ₃₄ O ₂	0.5	C16:0	236.2137	C ₁₆ H ₂₈ O	0.3
C ₄₂ H ₈₁ N ₂ O ₅	693	34.9	C18:1	282.2546	C ₁₈ H ₃₄ O ₂	1.3	C17:0	250.2291	C ₁₇ H ₃₀ O	0.6
C ₄₃ H ₈₃ N ₂ O ₅	707	5.1	C18:1	282.2540	C ₁₈ H ₃₄ O ₂	1.9	C18:0	264.2447	C ₁₈ H ₃₂ O	0.6
I (MMO) [M+H] ⁺										
C ₃₈ H ₇₃ N ₂ O ₅	637	18.3	C16:1	254.2251	C ₁₆ H ₃₀ O ₂	0.5	C16:0	236.2138	C ₁₆ H ₂₈ O	0.2
C ₃₉ H ₇₅ N ₂ O ₅	651	25.0	C16:1	254.2255	C ₁₆ H ₃₀ O ₂	0.9	C17:0	250.2294	C ₁₇ H ₃₀ O	0.3
C ₄₀ H ₇₇ N ₂ O ₅	665	5.6	C16:1	254.2261	C ₁₆ H ₃₀ O ₂	1.5	C18:0	264.2449	C ₁₈ H ₃₂ O	0.4
C ₄₀ H ₇₇ N ₂ O ₅	665	11.7	C18:1	282.2577	C ₁₈ H ₃₄ O ₂	1.8	C16:0	236.2138	C ₁₆ H ₂₈ O	0.2
C ₄₁ H ₇₉ N ₂ O ₅	679	27.7	C18:1	282.2559	C ₁₈ H ₃₄ O ₂	>0.1	C17:0	250.2293	C ₁₇ H ₃₀ O	0.4
C ₄₂ H ₈₁ N ₂ O ₅	693	11.8	C18:1	282.2567	C ₁₈ H ₃₄ O ₂	0.8	C18:0	264.2448	C ₁₈ H ₃₂ O	0.5



III (TMO) ^A Obs. Loss			Obs. Prod.		Obs. Prod.		Obs. Prod.		Obs. Prod.	
M ⁺	C ₃ H ₉ N	Δ mmu	C ₅ H ₁₀ NO ₂	Δ mmu	Obs. Prod.	Δ mmu	Obs. Prod.	Δ mmu	Obs. Prod.	Δ mmu
665	59.0737	0.2	116.0710	0.2	-	-	-	-	-	-
679	59.0731	0.4	116.0710	0.2	-	-	-	-	-	-
693	59.0735	>0.1	116.0709	0.3	-	-	-	-	-	-
693	59.0742	0.7	116.0709	0.3	-	-	-	-	-	-
707	59.0739	0.4	116.0710	0.2	-	-	-	-	-	-
721	59.0733	0.2	116.0710	0.2	-	-	-	-	-	-
II (DMO)										
[M+H] ⁺	C ₂ H ₇ N		C ₅ H ₁₀ NO ₂		C ₇ H ₁₄ NO ₂		C ₇ H ₁₇ N ₂ O ₂		C ₈ H ₁₅ N ₂ O ₃	
651	45.0582	0.4	116.0710	0.2	144.1020	0.5	161.1285	0.5	187.1079	0.4
665	45.0575	0.3	116.0710	0.2	144.1020	0.5	161.1285	0.5	187.1077	0.6
679	45.0574	0.4	116.0710	0.2	144.1021	0.4	161.1285	0.5	187.1078	0.5
679	45.0574	0.4	116.0710	0.2	144.1021	0.4	161.1285	0.5	187.1078	0.5
693	45.0578	>0.1	116.0710	0.2	144.1021	0.4	161.1285	0.5	187.1078	0.5
707	45.0578	>0.1	116.0710	0.2	144.1021	0.4	161.1285	0.5	187.1078	0.5
I (MMO)										
[M+H] ⁺	CH ₅ N		C ₅ H ₁₀ NO ₂		C ₆ H ₁₃ N ₂ O		C ₆ H ₁₅ N ₂ O ₂		C ₇ H ₁₃ N ₂ O ₃	
637	31.0422	>0.1	116.0710	0.2	129.1024	0.4	147.1129	0.5	173.0921	0.5
651	31.0428	0.6	116.0710	0.2	129.1024	0.4	147.1129	0.5	173.0923	0.3
665	31.0422	>0.1	116.0710	0.2	129.1024	0.4	147.1129	0.5	173.0922	0.4
665	31.0417	0.5	116.0710	0.2	129.1024	0.4	147.1129	0.5	173.0922	0.4
679	31.0427	0.5	116.0710	0.2	129.1024	0.4	147.1129	0.5	173.0923	0.3
693	31.0422	>0.1	116.0709	0.3	129.1023	0.5	147.1128	0.6	173.0920	0.6



Position	Trimethyl Ornithine			Ornithine		
	CH ₃	CH ₂	CH	CH ₃	CH ₂	CH
ϵ -N(CH ₃) ₃		53.8				
ϵ -NH ₂		-				5.71
δ		66.1		41.8		3.37
γ		19.2		21.9		1.96
β		29.9		27.9		2.62
β'		29.9		27.9		1.53
α			53.1		50.9	4.29
α -NH		-		-		6.54
2		41.9		42.0		2.51
3			71.5		71.3	5.21
4		34.8		34.1		1.62
5- ω 2		29.6		29.2		1.29
ω 1	22.5			22.5		0.88
2'		34.7		34.2		2.30
3'		25.1		25.1		1.62
8'- ω 2		29.6		29.6		1.29
ω 1'	22.5			22.5		0.88
DB		129.5		-		-
Adj-DB		27.4		-		-